The Effect of pH on Quercetin Release from Zn Crosslinked Chitosan-Alginate Membrane and Its Kinetics

Budi Hastuti[1*], Tejayani Nurroudhlotiningtyas[2], Saptono Hadi[2], and Mutiah Martanisa[1]

[1]*Department of Chemistry Education, Faculty of Teacher Training and Education, Universitas Sebelas Maret, Jl. Ir. Sutami 36A, Surakarta 57126, Indonesia*

[2]*Department of Pharmacy, Faculty of Mathematics and Natural Sciences, Universitas Sebelas Maret, Jl. Ir. Sutami 36A, Surakarta 57126, Indonesia*

* ***Corresponding author:***

tel: +62-8121504044
email: budihastuti@staff.uns.ac.id

Received: January 21, 2025
Accepted: October 22, 2025

DOI: 10.22146/ijc.104072

Abstract: *This research aims to assess the ability of Zn-crosslinked chitosan (Chi) and alginate (AG) membranes to deliver quercetin into the body by testing the release with variations in the pH of the dissolution medium. Chi-AG membrane crosslinked with Zn and loaded with quercetin to produce Chi-AG-Zn membrane with tear-resistant and elastic properties. The FTIR spectrum of the Zn crosslinked Chi-AG membrane containing quercetin shows the formation of a Chi-AG-Zn membrane with a shift in the characteristic peaks and the formation of new characteristic groups, namely Zn at a wavelength of 549 cm^{-1} and phenol at 1379 cm^{-1}. SEM testing showed that the surface of the fibrous membrane and quercetin were successfully loaded. Entrapment efficiency testing yielded relatively high results, specifically 91 ± 0.08%. The release of quercetin from the Zn-crosslinked Chi-AG membrane was investigated by varying the pH of the dissolution medium, specifically at pH 1.2, 5.0, and 7.4. The results showed the highest release at pH 7.4. Membrane release follows the Korsmeyer-Peppas model, and the release mechanism is governed by Fick's diffusion. These findings suggest that the Zn-crosslinked Chi-AG membrane has potential as a pH-responsive drug delivery system for targeted release in intestinal conditions.*

Keywords: *chitosan; alginate; Zn; quercetin; Zn-crosslinked Chi-AG membrane; drug release*

■ INTRODUCTION

Quercetin is a polyphenolic flavonoid compound that is abundantly available in nature, found in almost all parts of the plant, including seeds, leaves, stems, flowers, and leaves, especially in fruits and vegetables [1]. Quercetin exhibits high antioxidant activity, which can reduce the risk of degenerative diseases, including heart disease, osteoporosis, diabetes, hypertension, and cancer [2-5]. Quercetin is classified in the Biopharmaceutical Classification System (BCS) as class II, indicating that quercetin has high permeability but low solubility [6]. Quercetin is a lipophilic compound with poor physicochemical properties, including very low water solubility, being practically insoluble in water, poor bioavailability, a low absorption rate, and rapid elimination [7-8]. A drug can provide pharmacological effects when the compounds in the drug are released from the carrier substance, and one of the factors that affects the release of drug compounds is solubility [9].

Chitosan (Chi) is a biopolymer derived from deacetylated chitin, possessing biocompatible, biodegradable, and non-toxic properties. Chi has the ability to form films [10]. Chi contains two functional groups, namely hydroxyl and amine groups, which confer the biopolymer polycationic properties and high chemical reactivity. Chi nanoparticles offer several advantages, including enhanced stability, improved cellular uptake, increased solubility of anticancer drugs, modulation of release kinetics, and altered biodistribution [11]. Chi can be used as a drug matrix;

however, in acidic media, chitosan is soluble and may aggregate [12]. Its low solubility in water and poor mechanical properties necessitate modifications to increase its solubility, making it suitable for tissue engineering and drug delivery applications [13]. Chi has been developed into a multifunctional drug delivery system by exploring positively charged properties and modifiable functional groups [14]. Alginate (AG) and Chi, both biocompatible polymers, are crosslinked to enhance the gel's stability and mechanical strength [15].

Crosslinked membrane formation can increase the solubility of quercetin [16]. Modification of Chi and AG polyelectrolyte matrix with Zn crosslinking can strengthen the polymer and prevent degradation [17]. Chi can be used as a quercetin carrier matrix in drug delivery systems because it has good film-forming ability, good mucoadhesive, bioadhesion, and permeability properties that can improve drug delivery, transportation, and release [18-21]. AG polymer is composed of a linear chain consisting of α-L-guluronate acid and β-D-mannuronate acid residues connected by a 1,4 bond. AG is widely used as a drug delivery matrix because it is safe, cheap, and has good mechanical strength [22]. AG can form gels, and it is governed mainly by the coordination of the number of cations. The role of cations in alginate gels is believed to be the shielding of electrostatic repulsion between anionic groups, such as carboxylate, and direct binding through ionic bonds [23]. The most distinctive ability of AG is its gelation through ionic interactions, influenced by various divalent and trivalent metal cations, such as Zn.

Transition metal oxides are used as crosslinkers in ionic reactions between molecules, as well as gelation enhancers for polymers to improve their basic properties, such as mechanical and thermal stability. Crosslinking between Zn and AG shows excellent prospects for drug loading at a sustained level over a long period, to act as a controlled drug delivery system [24-26]. AG contain many free hydroxyl (–OH) and carboxyl (–COOH) groups that enable them to form intramolecular hydrogen bonds [27]. When combined with Chi, a polycationic polymer, AG can form a polyelectrolyte complex through ionic interactions between amino groups in Chi and carboxyl groups in AG. When functioning as a matrix for immobilizing biomaterials, PEC has an advantage over its original polymers [28]. This complex exhibits high stability against pH changes and enhances encapsulation efficiency compared to using a single polymer [29]. Such properties make Chi-AG membranes highly promising for various biomedical applications.

Previous studies have developed Chi-AG membranes crosslinked with agents such as calcium ions or glutaraldehyde, which exhibited good film formation and controlled swelling behavior [30]. Additionally, an AG-Chi-based membrane hydrogel is also available, utilizing sodium tripolyphosphate (TPP) as a crosslinking agent [31]. Studies involving zinc ions (Zn^{2+}) as a crosslinker have primarily focused on AG hydrogels or AG films without Chi, and have indeed demonstrated antimicrobial activity and improved stability [32]. However, studies specifically utilizing Zn^{2+}-crosslinked Chi-AG membranes for drug delivery are still limited, particularly in assessing their performance at different physiological pH conditions. This study fills that gap by developing Zn^{2+} crosslinked Chi-AG membranes loaded with quercetin. The novelty lies in systematically evaluating how Zn^{2+} crosslinking influences membrane structure, mechanical stability, and pH-responsive release kinetics of quercetin.

■ EXPERIMENTAL SECTION

Materials

The materials used in this study were quercetin (Sigma Aldrich), technical Chi food grade, technical AG food grade, acetic acid (Mallinckrodt, USA), and distilled water. Additionally, $ZnCl_2$, sodium acetate, potassium dihydrogen phosphate, hydrochloric acid, ethanol, potassium chloride, and sodium hydroxide were supplied from Merck, Germany.

Instrumentation

The tools used in this study were a set of paddle-type dissolution apparatus (Biobase RC-6 Dissolution Tester; Tianjin, China), UV-vis spectrophotometer (Genesys 10s UV-vis; California, USA), Fourier-transform infrared (FTIR) spectrophotometer, scanning electron microscopy (SEM), X-ray diffractometer

(XRD), oven (Memmert: Schwabach, Germany), pH meter (Eutech pH 330: Illinois, USA), digital analytical balance (Sartorius, d=0.001; Gŏttingen, Germany), stirrer (Mtops MS300 Hs; Seoul, Korea), magnetic stirrer, stopwatch, and laboratory glassware (Pyrex; Corning, USA).

Procedure

A Chi-AG membrane was prepared by carefully weighing 0.763 g of Chi powder, which was then dissolved in 100 mL of a 2% CH_3COOH solution. The mixture was stirred at 1,000 rpm for 30 min at room temperature until the Chi was completely dissolved and then allowed to stand for 24 h. AG powder was carefully weighed to a mass of 0.396 g and then dissolved in 100 mL of a 2% CH_3COOH solution. The mixture was stirred at 1,000 rpm for 1 h at room temperature, until the AG was completely dissolved, and then allowed to stand for 24 h. Then, the solution was molded using plastic molds and oven-dried at 55 °C for approximately 40 h. The concentration of AG and Chi was selected based on preliminary trials to achieve uniform drug distribution and optimal mechanical strength of the membrane.

Zn crosslinked Chi-AG membrane loaded with quercetin was prepared by the solvent casting method. A $ZnCl_2$ solution of up to 5 mL was mixed with the AG solution that had been allowed to stand overnight. Then, a Chi solution was added and stirred at 1,000 rpm until homogeneous. Quercetin powder, weighing up to 25 mg, was weighed and then dissolved in 25 mL of ethanol. The quercetin solution was then mixed with the Chi-AG-Zn solution mixture and stirred at 1,000 rpm until a homogeneous mixture was achieved. Then, the solution was molded using plastic molds and oven-dried at 55 °C for approximately 20 h.

An entrapment efficiency (EE) test was conducted by preparing a series of calibration solutions in both ethanol media and buffer media with pH levels of 1.2, 5.0, and 7.4, and with concentrations of 2.0, 4.0, 6.0, 8.0, and 10 µg/mL. The absorbance was measured using a UV-vis spectrophotometer with the maximum wavelength obtained. Quercetin-loaded Zn-crosslinked Chi-AG membrane, weighing as much as 200 mg, was immersed in 96% ethanol for 24 h. The absorbance was then measured using a UV-vis spectrophotometer at the maximum wavelength of quercetin.

The quercetin release test from the membrane was conducted by carefully weighing the Zn-crosslinked Chi-AG membrane as much as 200 mg and then inserting it into the dissolution media of buffer solution: 96% ethanol (70:30 v/v) with pH variations of 1.2, 3.6, and 7.4 each, as much as 250 mL at a temperature of 37 ± 0.5 °C. The stirring speed was maintained at 75 rpm. The release of quercetin was measured at 0, 15, 30, 45, 60, 120, 180, and 240 min for 4 h by withdrawing 5 mL of dissolution media at each time point, maintaining the same pH and temperature. Furthermore, the solution was measured for absorbance using a UV-vis spectrophotometer at a maximum wavelength. All experiments were performed in duplicate (n = 2) to ensure data reproducibility.

Membrane characterization

FTIR characterization was carried out by the KBr pellet method. The sample was crushed and weighed carefully, ranging from 1 to 10 mg. It was then mixed with dry KBr powder, up to 100 mg, and the resulting mixture was molded into pellets. Furthermore, scanning was carried out at wavenumbers 400–5,000 cm^{-1}. SEM characterization was performed by placing the sample in a specimen holder that had been coated with a thin layer of platinum and then vacuum-sealed and inserted into the specimen chamber. Sample analysis was carried out at magnifications of 500×, 1000×, and 1500× with a voltage of 10 kV. Diffraction patterns of Zn crosslinked alginates-chitosan, chitosan, alginates, and alginates-chitosan were obtained using XRD. The samples were scanned using X-ray radiation with a monochromatic Cu $K\alpha_1$ source at a voltage of 50 kV and a current of 100 mA. The diffraction pattern was obtained at temperatures ranging from 10 to 70 °C with a diffraction angle of 2θ, a scanning speed of 5°/min, and a rate size of 0.02°/s [33].

■ RESULTS AND DISCUSSION

The characteristics of the Zn-crosslinked Chi-AG membrane based on organoleptic assessment are that the membrane appears transparent and slightly

yellowish in color with a characteristic acidic odor of acetic acid. The membrane has plastic-like surface properties and is slightly stiff. The membrane formed is sturdy and not easily torn, as shown in Fig. 1(a). The quercetin-loaded Zn-crosslinked Chi-AG membrane is marginally stiffer than the membrane that has not been loaded with quercetin. The membrane packed with quercetin is also bright yellow in color, typical of quercetin, as shown in Fig. 1(b).

Zn was added to act as a crosslinking agent that would bind to both polymers. Zn binds to the OH groups present in Chi and AG. The bond that occurs is a covalent bond where Zn shares an electron pair with each OH. Quercetin can be loaded onto the Chi-AG membrane, as shown in the proposed interaction in Fig. 2. The interaction between polycationic from Chi and polyanionic from AG is formed from the synthesis of Zn crosslinked Chi-AG membrane. The interaction occurs between the two polymers, namely OH^- from Chi and OH^- from AG, that have interacted with Zn^+ to form a Zn-crosslinked Chi-AG-PEC membrane. Chi and AG form covalent bonds as shown in Fig. 2(a). The loading of quercetin on the Zn-crosslinked Chi-AG membrane forms a new bond. Quercetin has an OH^- group that can bind to the NH_3^+ group present on the Zn-crosslinked Chi-AG. Hydrogen bonds are formed from OH^- quercetin interacting with OH^- AG on the Zn crosslinked Chi-AG by forming hydrogen bonds, as shown in Fig. 2(b).

Membrane Characterization

Fig. 3 shows the differences in characteristic peaks of functional groups found in Chi membranes, AG membranes, Zn-crosslinked Chi-AG membranes, and Zn-crosslinked Chi-AG membranes loaded with quercetin

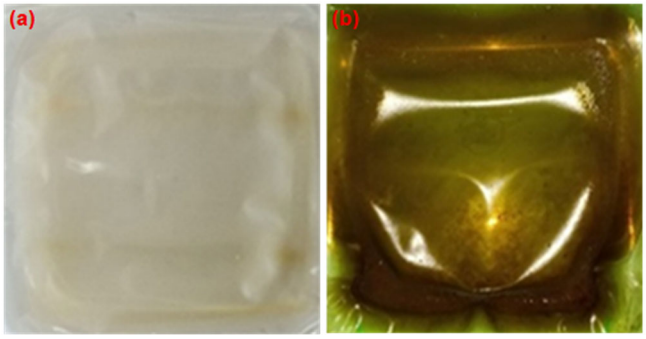

Fig 1. Membrane (a) Zn-crosslinked Chi-AG and (b) quercetin-loaded Zn-crosslinked Chi-AG

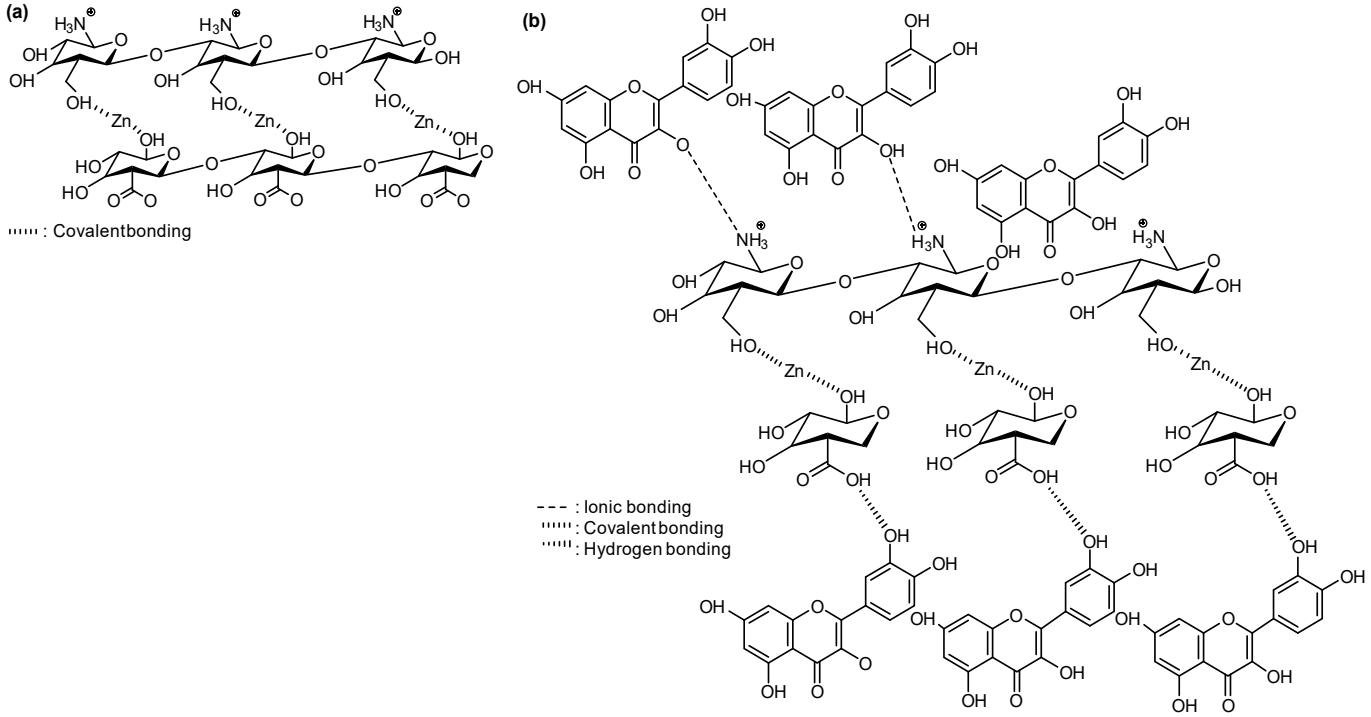

Fig 2. Proposed interaction of (a) Zn-crosslinked Chi-AG and (b) quercetin-loaded Zn-crosslinked Chi-AG

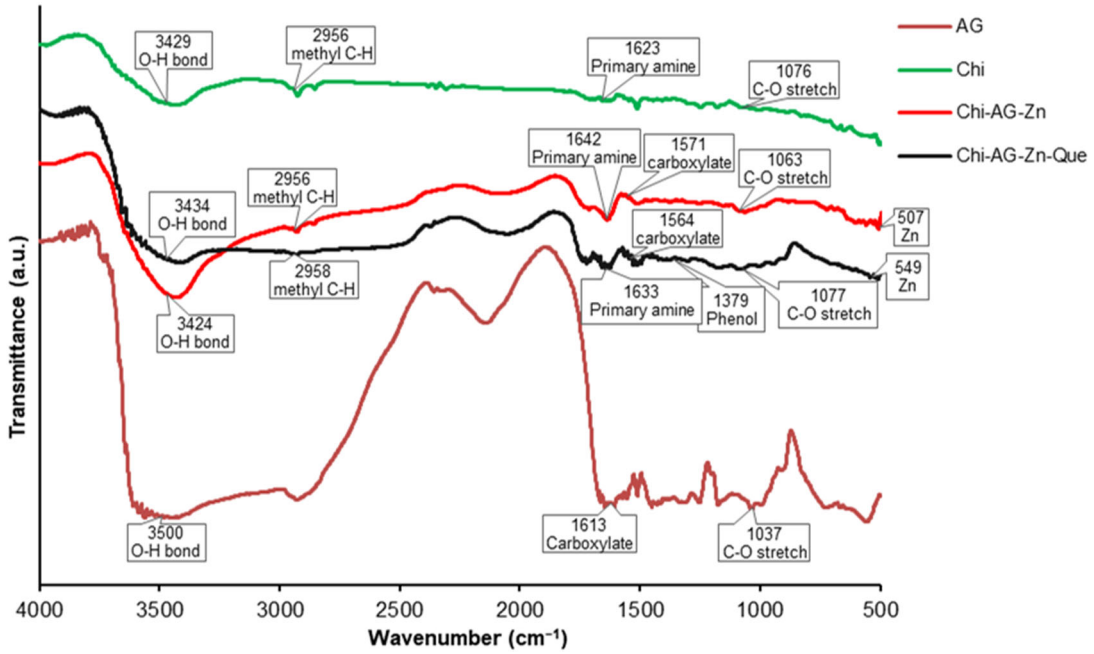

Fig 3. FTIR spectra of Chi, AG, Zn-crosslinked Chi-AG, and quercetin-loaded Zn-crosslinked Chi-AG membranes

that have been prepared. The interaction between Chi and AG is evident in the FTIR spectra, which exhibit several characteristic features, including wavelength shifts and intensity differences.

FTIR spectra show that the AG membrane shows absorption at 3500 cm^{-1}, which is the O–H stretch vibration. In contrast, the absorption of 2956 cm^{-1} is the vibration of the C–H group. In addition, there is absorption at 1420 and 1597 cm^{-1}, which correspond to symmetrical C=O group vibration and asymmetrical C=O, respectively. A signal at 1037 cm^{-1} shows C–O–C stretch vibration. The FTIR spectrum of the Chi-AG membrane shows that the absorption at a wavenumber of 3449 cm^{-1} corresponds to the vibration of the O–H group, in addition to the C–H vibration appearing at a wavenumber of 2956 cm^{-1}. The absorption at 1643 cm^{-1} is the characteristic absorption of the asymmetrical C=O group of AG [34] and 1571 cm^{-1} is the characteristic absorption of the N–H group from Chi. The C=O group of AG and the amine group of Chi that still appear on the FTIR spectrum of the Chi-AG membrane show that what occurs in the formation of the Chi-AG membrane.

The interaction between Chi and AG forms a polyelectrolyte complex which can be seen from the shift in the number of waves of the N–H group from 1582 to 1528 cm^{-1} and the C=O group which shifts from 1597 to 1636 cm^{-1} in addition to the change in intensity in the FTIR spectrum of the Chi-AG membrane when compared to the FTIR spectrum of individual Chi and AG. Chi exhibits an absorption band that is distinct from AG, specifically in the absorption region at a wavenumber of 1623 cm^{-1}, indicating the presence of a primary N–H group. The characteristics that distinguish alginate from chitosan include the presence of a–COOH group at 1613 cm^{-1} [35].

Zn crosslinking is characterized by a characteristic peak at 507 cm^{-1}. FTIR spectra of the membranes confirmed the interaction between AG, Chi, and Zn^{2+}. The characteristic absorption band of AG at 1634 cm^{-1} (asymmetric stretching of $–COO^-$) shifted to a lower wavenumber upon crosslinking, indicating ionic interaction with the protonated amine groups ($–NH_3^+$) of Chi and coordination with Zn^{2+} ions. Similarly, the peak at 3434 cm^{-1}, corresponding to O–H and N–H stretching, became broader and less intense, suggesting hydrogen bonding and partial involvement of O–H groups in crosslinking [36]. These spectral changes support the formation of Zn^{2+}-crosslinked membranes, making the Chi-AG structure more stable and organized.

The inclusion of quercetin in the Zn-crosslinked Chi-AG membrane is evident from the FTIR spectra, which exhibit several characteristic features, including wavelength shifts and intensity differences. The absorption intensity of the wavelength of each membrane changes so that there is a difference in the intensity of the Zn-crosslinked Chi-AG membrane and the quercetin-loaded Zn-crosslinked Chi-AG membrane. There is a phenol peak at 1379 cm^{-1}, which is characteristic of quercetin. This can indicate that the membrane was successfully loaded with quercetin. The surface morphology of the membrane can be characterized using SEM.

The maximum magnification of SEM testing can be achieved at 1500×. The Chi membrane (Fig. 4(a)) appears to have a surface that is more fibrous than that of the AG membrane. The AG membrane (Fig. 4(b)) seems to have a smoother surface than the Chi membrane. Fig. 4(c) shows the surface morphology of the Chi-AG-Zn membrane, which is rough and porous. These results are similar to those of previous studies, which reported that AG-Chi membranes exhibit a rough and porous inner surface structure [37]. Surface roughness is an important feature associated with cell adhesion and proliferation [38].

Zn on Chi-AG membrane crosslinked Zn-loaded quercetin appears more evenly distributed compared to Zn on Chi-AG membrane crosslinked Zn. Quercetin on the quercetin-loaded Zn-crosslinked Chi-AG membrane appears successfully loaded as shown in Fig. 4(d). The large number of pores in the chitosan alginate membrane has the potential to encapsulate large quantities of quercetin. The ionic bond between Chi and AG breaks the close packing of Chi to form a crystal structure, so that Chi-AG membrane is more stable when compared to the pure compound. The pore size on the surface of microparticles significantly influences the release rate of encapsulated substances. Microparticles with larger pores allow for faster release of active ingredients, while smaller pores tend to slow down the process [36].

XRD analysis was performed to determine the crystallinity of AG, Chi, Chi-AG, and Chi-AG membranes crosslinked with Zn. The results are shown in Fig. 5. The AG's spectrum shows high crystallinity [39].

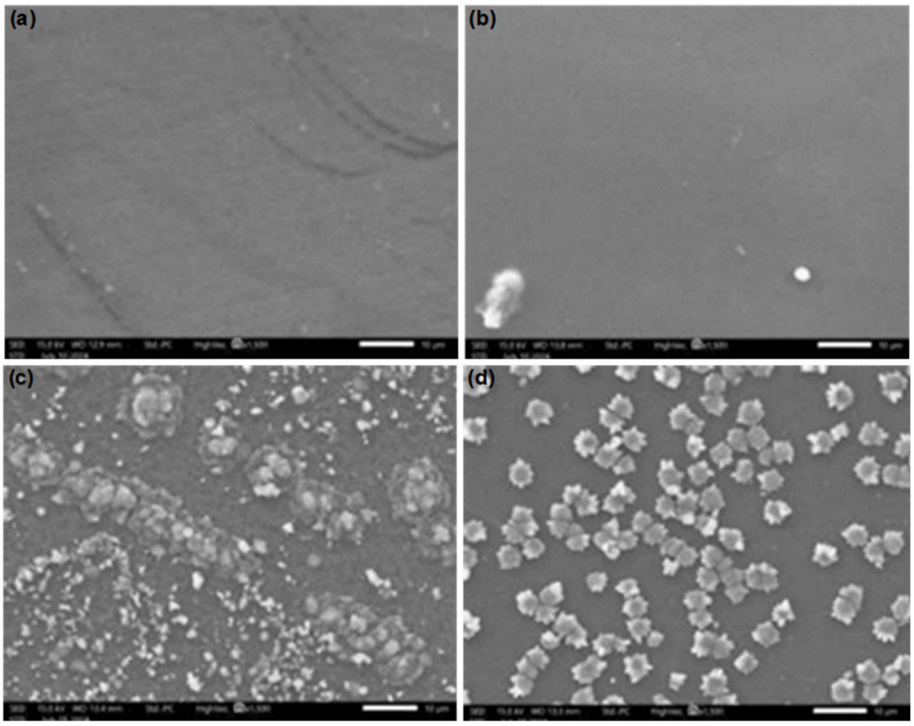

Fig 4. SEM analysis results with 1500× magnification of (a) Chi membrane, (b) AG membrane, (c) Zn-crosslinked Chi-AG membrane, and (d) Zn-crosslinked Chi-AG membrane loaded with quercetin

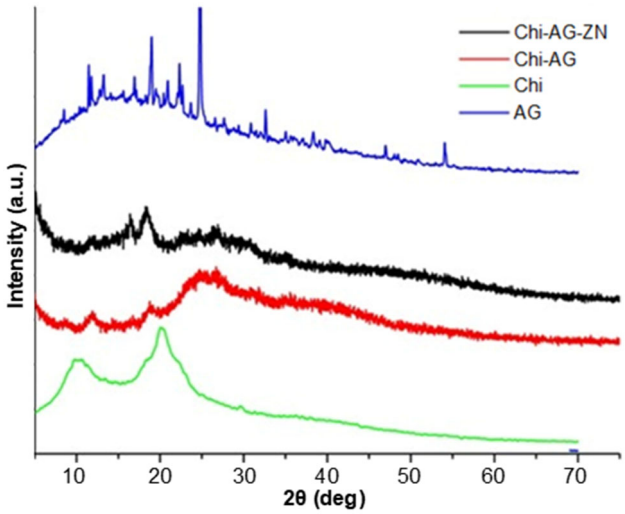

Fig 5. XRD analysis results of AG, Chi, Chi-AG, and Zn-crosslinked Chi-AG

Based on Fig. 5, it is known that the XRD results of AG have several sharp peaks. While Chi is semi-crystalline, as indicated by two broad peaks. Fig. 5, in green, is an XRD spectrum of Chi, indicating that it is semicrystalline, as evidenced by the presence of peaks at 2θ = 12° and 22°. When AG and Chi are crosslinked with Zn, they exhibit lower intensity peaks than pure AG and Chi. This indicates that the crystallinity properties decrease due to the crosslinking process. The red color Chi-AG XRD spectrum shows a combination of properties of Chi and AG; the greater amount of AG on the membrane causes a more amorphous structure.

The membrane of Chi-AG-Zn (black color) is more similar to the structure of Chi-AG (red color), which shows more amorphous. The presence of AG in the Chi membrane of alginate-Zn causes a decrease in the crystallinity level of Chi or AG. This can be observed from the disappearance of 2θ at 12° after the formation of the AG-Chi polyelectrolyte complex. The formation of the Chi-AG membrane broke the hydrogen bonding between amino and hydroxyl groups in Chi. Then it resulted in an amorphous structure of the Chi-AG complex. The decreased crystallinity of the Chi-AG membrane also implied that the ionic interaction between Chi and AG led to their good compatibility [35].

Amorphous solids lack the repeating array of atoms in the structure and present greater free energy than their crystalline counterparts, which in turn enhances the solubility of the compound. The loading of drug compounds into porous materials has been described as a promising approach for stabilizing the amorphous state, but it is dependent on many factors, including the pore size and surface chemistry of the substrate material [40]. The determination of the percentage of quercetin rerelease in the solution medium was determined using a UV Vis spectrophotometer by observing the wavelength of the visible light region of 300–500 nm. Quercetin has chromophore and auxochrome groups, which provide color absorption in the visible light wavelength region.

The release profile of quercetin from Zn-crosslinked Chi-AG membrane was obtained by conducting a dissolution test. The dissolution test is an *in vitro* test used to determine the percentage of a drug that is distributed into the body. The dissolution test was conducted by preparing a 200 mg sample of Zn-crosslinked Chi-AG membrane for each dissolution medium. The release test used a paddle-type dissolution apparatus with modifications. The dissolution media used were made in pH variations of 1.2, 5.0, and 7.4 with a mixture of pH buffer: ethanol (70:30). Each pH describes the conditions in body fluids; pH 1.2 describes the acidic conditions of the stomach, pH 5.0 describes the conditions of the small intestine, and pH 7.4 describes the conditions in the human large intestine.

The release profile of quercetin from Zn-crosslinked Chi-AG membranes at several medium pH levels can be seen in Fig. 6. The dissolution medium used included simulations of gastric pH (pH 1.2), intestinal pH (pH 5.0), and pH 7.4. The release profile of quercetin from Zn-crosslinked Chi-AG membranes appeared to increase, followed by a relatively stable release even in dissolution media with different pH. The release profile showed that the amount of quercetin released increased as the pH of the dissolution media increased. The percentage of quercetin released in the dissolution medium at pH 1.2, pH 5.0, and pH 7.4 from the membrane was 35.1059, 70.2783, and 94.3471%, respectively. The highest release was observed in dissolution media with a pH of 7.4, and the lowest was in pH 1.2. This is because the pH of the

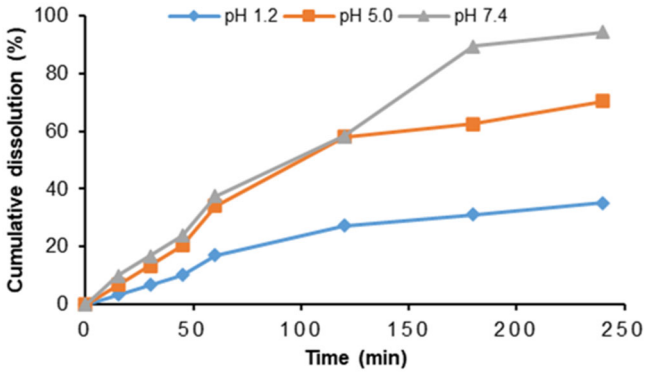

Fig 6. Release profile of quercetin from Zn-crosslinked Chi-AG membrane

solvent can affect the ionic interaction between NH_3^+ from Chi and OH^- from AG, as well as the interaction between OH^- from quercetin and the solvent. Quercetin is weakly acidic, and in an environment with a higher pH, it will be more ionized. The electrostatic bond will weaken when the pH decreases or the atmosphere is more acidic. If the electrostatic bond decreases, the membrane will expand slowly. Adding AG and Zn can prevent acid-soluble Chi, ensuring the membrane surface does not extend at low pH, which can cause quercetin to be released from the membrane. This can prevent quercetin from being released at low pH levels when consumed, such as in the stomach, allowing quercetin to avoid degradation by stomach acid and provide more benefits.

Table 1 shows that the kinetics of quercetin release from Zn-crosslinked Chi-AG membranes at all pH variations follow the Korsmeyer-Peppas model. Korsmeyer-Peppas model is used to describe drug release from a polymeric system, considering non-Fickian mechanisms [41]. The first-order model assumes that the release rate is either constant or directly dependent on the concentration [42]. Theoretically, the Higuchi model cannot be used to analyze swellable drug delivery systems [38]. Therefore, both are often unable to describe the non-linear release profiles that arise in crosslinked polymer matrices, where diffusion, swelling, and/or erosion mechanisms can simultaneously influence the release rate. On the contrary, non-linear equations coming from Korsmeyer-Peppas and Weibull models better fit the release profiles [43].

The r^2 value of each release of Zn-crosslinked Chi-AG membrane with pH variations of 1.2, 5.0, and 7.4 were 0.9635, 0.9598, and 0.9889, respectively, with quercetin release rate based on the release constant of 2.3795, 2.3938, and 2.3393 min^{-1}, respectively. The value of n (exponent) indicates the mechanism of release. The value of n in each pH variation of the release was at the value of $n < 0.5$, which means the release of quercetin from Zn-crosslinked Chi-AG membrane follows the Fick diffusion mechanism, which describes the mechanism of drug release from a non-swellable matrix, so that the release of quercetin from Chi-AG-Zn membrane through diffusion from high concentration to lower concentration [44].

The dense polymer network formed by Zn^{2+} crosslinking limits chain mobility and reduces pore size, thereby controlling the diffusion of drugs. Under conditions that mimic the *in vivo* environment, this diffusion-based release mechanism is advantageous because it can maintain prolonged quercetin availability and reduce the initial release (burst) effect, thereby enhancing therapeutic efficiency and reducing the need

Table 1. Results of quercetin release testing of Zn-crosslinked Chi-AG membrane

pH	Parameters	Zero Order	First Order	Higuchi	Korsmeyer-Peppas	
1.2	r^2	0.9255	0.7522	0.9557	0,9635	Fick diffusion ($n < 0.5$)
	k	0.0030	0.0039	0.0256	2.3795	
	n	-	-	-	0.3765	
5.0	r^2	0.9112	0.7446	0.9470	0.9598	Fick diffusion ($n < 0.5$)
	k	0.0060	0.0039	0.0519	2.3938	
	n	-	-	-	0.3791	
7.4	r^2	0.9676	0.8483	0.9496	0.9889	Fick diffusion ($n < 0.5$)
	k	0.0080	0.0040	0.0683	2.3393	
	n	-	-	-	0.3691	

for frequent dosing. Burst release is often considered an adverse effect when considering long-term drug delivery systems. This burst release effect leads to negative consequences, such as local toxicity from high drug concentrations, requiring more frequent dosing, and economically and therapeutically wasting the drug. Crosslinking has been shown to improve network stability and prevent burst release [45]. The complexation of Chi with AG reduces the burst release behavior. This reduction is due to a decrease in voids in the AG polymer network. The low voids in the polymer network reduce swelling and thus prevent burst release [38].

■ CONCLUSION

The pH variation of the dissolution medium affects the release of quercetin from the Zn-crosslinked Chi-AG membrane. The higher the pH of the dissolution medium, the faster the release of quercetin from the Zn-crosslinked Chi-AG membrane. This is because quercetin is weakly acidic, and when in an environment with a higher pH, quercetin will be more ionized. The release of quercetin from the Zn-crosslinked Chi-AG membrane, in response to variations in the dissolution medium, follows the Korsmeyer-Peppas kinetics model, with the release mechanism described by Fick's diffusion, which characterizes the release of drugs from non-swellable membranes. Overall, Zn^{2+} crosslinking enhanced membrane stability and enabled sustained release of quercetin, highlighting its potential as a pH-responsive delivery platform for poorly soluble bioactive compounds. However, this study was limited to *in vitro* characterization and release evaluation under simplified conditions. Further studies are recommended to assess the *in vitro-in vivo* correlation and optimize crosslinking parameters for targeted therapeutic applications.

■ ACKNOWLEDGMENTS

The authors thank the Institute for Research and Community Service of Universitas Sebelas Maret (LPPM UNS) for providing financial support to the research through the Fundamental Research Grant.

■ CONFLICT OF INTEREST

There is no conflict of interest to be declared.

■ AUTHOR CONTRIBUTIONS

Budi Hastuti conducted the experiments, conceived and designed the experiments, provided reagents and materials, and was responsible for data analysis and interpretation. Tejayani Nurroudhlotiningtyas performed the experimental work, contributed to data analysis, and drafted the manuscript. Saptono Hadi participated in the experimental work and contributed to manuscript preparation. Mutiah Martanisa participated in the process of making and editing graphic data. All authors reviewed and agreed to the final version of this manuscript.

■ REFERENCES

[1] Xu, D., Hu, M.J., Wang, Y.Q., and Cui, Y.L., 2019, Antioxidant activities of quercetin and its complexes for medicinal application, *Molecules*, 24 (6), 1123.

[2] Uthra, C., Shrivastava, S., Jaswal, A., Sinha, N., Reshi, M.S., and Shukla, S., 2017, Therapeutic potential of quercetin against acrylamide induced toxicity in rats, *Biomed. Pharmacother.*, 86, 705–714.

[3] Patel, R.V., Mistry, B.M., Shinde, S.K., Syed, R., Singh, V., and Shin, H.S., 2018, Therapeutic potential of quercetin as a cardiovascular agent, *Eur. J. Med. Chem.*, 155, 889–904.

[4] Jakaria, M., Azam, S., Jo, S.H., Kim, I.S., Dash, R., and Choi, D.K., 2019, Potential therapeutic targets of quercetin and its derivatives: Its role in the therapy of cognitive impairment, *J. Clin. Med.*, 8 (11), 1789.

[5] Rifaai, R.A., Mokhemer, S.A., Saber, E.A., Abd El-Aleem, S.A., and El-Tahawy, N.F.G., 2020, Neuroprotective effect of quercetin nanoparticles: A possible prophylactic and therapeutic role in Alzheimer's disease, *J. Chem. Neuroanat.*, 107, 101795.

[6] Mu, Y., Fu, Y., Li, J., Yu, X., Li, Y., Wang, Y., Wu, X., Zhang, K., Kong, M., Feng, C., and Chen, X., 2019, Multifunctional quercetin conjugated chitosan nano-micelles with P-gp inhibition and

permeation enhancement of anticancer drug, *Carbohydr. Polym.*, 203, 10–18.

[7] Kaşıkcı, M.B., and Bağdatlıoğlu, N., 2016, Bioavailability of quercetin, *Curr. Res. Nutr. Food Sci.*, 4 (SI. 2), 146–151.

[8] Gilley, A.D., Arca, H.C., Nichols, B.L.B., Mosquera-Giraldo, L.I., Taylor, L.S., Edgar, K.J., and Neilson, A.P., 2017, Novel cellulose-based amorphous solid dispersions enhance quercetin solution concentrations *in vitro*, *Carbohydr. Polym.*, 157, 86–93.

[9] van der Merwe, J., Steenekamp, J., Steyn, D., and Hamman, J., 2020, The role of functional excipients in solid oral dosage forms to overcome poor drug dissolution and bioavailability, *Pharmaceutics*, 12 (5), 393.

[10] Das, A., Ghosh, S., and Pramanik, N., 2024, Chitosan biopolymer and its composites: Processing, properties and applications- A comprehensive review, *Hybrid Adv.*, 6, 100265

[11] Grewal, A.K., and Salar, R.K., 2024, Chitosan nanoparticle delivery systems: An effective approach to enhancing efficacy and safety of anticancer drugs, *Nano TransMed*, 3, 100040.

[12] Yadav, H., Malviya, R., and Kaushik, N., 2024, Chitosan in biomedicine: A comprehensive review of recent developments, *Carbohydr. Polym. Technol. Appl.*, 8 (2), 100551.

[13] Desai, N., Rana, D., Salave, S., Gupta, R., Patel, P., Karunakaran, B., Sharma, A., Giri, J., Benival, D., and Kommineni, N., 2023, Chitosan: A potential biopolymer in drug delivery and biomedical applications, *Pharmaceutics*, 15 (4), 1313.

[14] Herdiana, Y., Wathoni, N., Shamsuddin, S., and Muchtaridi, M., 2022, Drug release study of the chitosan-based nanoparticles, *Heliyon*, 8 (1), e08674.

[15] Bustos, D., Guzmán, L., Valdés, O., Muñoz-Vera, M., Morales-Quintana, L., and Castro, R.I., 2023, Development and evaluation of cross-linked alginate–chitosan–abscisic acid blend gel, *Polymers*, 15 (15), 3217.

[16] Kawabata, K., Mukai, R., and Ishisaka, A., 2015, Quercetin and related polyphenols: New insights and implications for their bioactivity and bioavailability, *Food Funct.*, 6 (5), 1399–1417.

[17] Hasnain, M.S., and Nayak, A.K., 2018, "Alginate-inorganic composite particles as sustained drug delivery matrices" in *Applications of Nanocomposite Materials in Drug Delivery, Woodhead Publishing Series in Biomaterials*, Eds. Inamuddin, I., Asiri, A.M., and Mohammad, A., Woodhead Publishing, Sawston, Cambridge, UK, 39–74.

[18] Yu, J., Wang, J., and Jiang, Y., 2017, Removal of uranium from aqueous solution by alginate beads, *Nucl. Eng. Technol.*, 49 (3), 534–540.

[19] Ewart, D., Peterson, E.J., and Steer, C.J., 2019, A new era of genetic engineering for autoimmune and inflammatory diseases, *Semin. Arthritis Rheum.*, 49 (1), e1–e7.

[20] Shamsi, M., Mohammadi, A., Manshadi, M.K.D., and Sanati-Nezhad, A., 2019, Mathematical and computational modeling of nano-engineered drug delivery systems, *J. Controlled Release*, 307, 150–165.

[21] Su, C., Liu, Y., Li, R., Wu, W., Fawcett, J.P., and Gu, J., 2019, Absorption, distribution, metabolism and excretion of the biomaterials used in nanocarrier drug delivery systems, *Adv. Drug Delivery Rev.*, 143, 97–114.

[22] Sugiono, S., Masruri, M., Estiasih, T., and Widjarnako, S.B., 2019, Structural and rheological characteristics of alginate from *Sargassum cristaefolium* extracted by twin screw extruder, *J. Aquat. Food Prod. Technol.*, 28 (9), 944–959.

[23] Hu, C., Lu, W., Mata, A., Nishinari, K., and Fang, Y., 2021, Ions-induced gelation of alginate: Mechanisms and applications, *Int. J. Biol. Macromol.*, 177, 578–588.

[24] Aquino, R.P., Auriemma, G., and Cerciello, A., 2017, "NSAIDS: Design and Development of Innovative Oral Delivery Systems" in *Nonsteroidal Anti-Inflammatory Drugs*, Eds. Al-Kaf, A.G., IntechOpen, London, UK.

[25] Rodríguez-Dorado, R., López-Iglesias, C., García-González, C.A., Auriemma, G., Aquino, R.P., and Del Gaudio, P., 2019, Design of aerogels, cryogels

and xerogels of alginate: Effect of molecular weight, gelation conditions and drying method on particles' micromeritics, *Molecules*, 24 (6), 1049.

[26] Priyadarshi, R., Kumar, B., and Rhim, J.W., 2020, Green and facile synthesis of carboxymethylcellulose/ZnO nanocomposite hydrogels crosslinked with Zn^{2+} ions, *Int. J. Biol. Macromol.*, 162, 229–235.

[27] Fernando, I.P.S., Lee, W.W., Han, E.J., and Ahn, G., 2020, Alginate-based nanomaterials: Fabrication techniques, properties, and applications, *Chem. Eng. J.*, 391, 123823.

[28] Fernando, I.P.S., Lee, W.W., Han, E.J., and Ahn, G., 2020, Alginate-based nanomaterials: Fabrication techniques, properties, and applications, *Chem. Eng. J.*, 391, 123823.

[29] Atma, Y., Sadeghpour, A., Murray, B.S., and Goycoolea, F.M., 2025, Chitosan-alginate polyelectrolyte complexes for encapsulation of low molecular weight fish bioactive peptides, *Food Hydrocolloids*, 160, 110789.

[30] Jiang, C., Wang, Z., Zhang, X., Zhu, X., Nie, J., and Ma, G., 2014, Crosslinked polyelectrolyte complex fiber membrane based on chitosan–sodium alginate by freeze-drying, *RSC Adv.*, 4 (78), 41551–41560.

[31] Gierszewska, M., Ostrowska-Czubenko, J., and Chrzanowska, E., 2018, pH-responsive chitosan/alginate polyelectrolyte complex membranes reinforced by tripolyphosphate, *Eur. Polym. J.*, 101, 282–290.

[32] Cano-Vicent, A., Tuñón-Molina, A., Bakshi, H., Sabater i Serra, R., Alfagih, I.M., Tambuwala, M.M., and Serrano-Aroca, Á., 2023, Biocompatible alginate film crosslinked with Ca^{2+} and Zn^{2+} possesses antibacterial, antiviral, and anticancer activities, *ACS Omega*, 8 (27), 24396–24405.

[33] Yousaf, A.M., Malik, U.R., Shahzad, Y., Mahmood, T., and Hussain, T., 2019, Silymarin-laden PVP-PEG polymeric composite for enhanced aqueous solubility and dissolution rate: Preparation and *in vitro* characterization, *J. Pharm. Anal.*, 9 (1), 34–39.

[34] Belattmania, Z., Kaidi, S., El Atouani, S., Katif, C., Bentiss, F., Jama, C., Reani, A., Sabour, B., and Vasconcelos, V., 2020, Isolation and FTIR-ATR and ^{1}H NMR characterization of alginates from the main alginophyte species of the Atlantic coast of Morocco, *Molecules*, 25 (18), 4335.

[35] Wang, G., Wang, X., and Huang, L., 2017, Feasibility of chitosan-alginate (Chi-Alg) hydrogel used as scaffold for neural tissue engineering: A pilot study *in vitro*, *Biotechnol. Biotechnol. Equip.*, 31 (4), 766–773.

[36] Vinceković, M., Jurić, S., Vlahoviček-Kahlina, K., Martinko, K., Šegota, S., Marijan, M., Krčelić, A., Svečnjak, L., Majdak, M., Nemet, I., Rončević, S., and Rezić, I., 2023, Novel zinc/silver ions-loaded alginate/chitosan microparticles antifungal activity against *Botrytis cinerea*, *Polymers*, 15 (22), 4359.

[37] Wijaya, A.R., Syah, A.A., Hana, D.C., and Putra, H.F.S., 2024, Addition of chitosan to calcium-alginate membranes for seawater NaCl adsorption, *AIMS Environ. Sci.*, 11 (1), 75–89.

[38] Unagolla, J.M., and Jayasuriya, A.C., 2018, Drug transport mechanisms and *in vitro* release kinetics of vancomycin encapsulated chitosan-alginate polyelectrolyte microparticles as a controlled drug delivery system, *Eur. J. Pharm. Sci.*, 114, 199–209.

[39] Feyissa, Z., Edossa, G.D., Gupta, N.K., and Negera, D., 2023, Development of double crosslinked sodium alginate/chitosan based hydrogels for controlled release of metronidazole and its antibacterial activity, *Heliyon*, 9 (9), e20144.

[40] Jones, E.C.L., and Bimbo, L.M., 2020, Crystallisation behaviour of pharmaceutical compounds confined within mesoporous silicon, *Pharmaceutics*, 12 (3), 214.

[41] Heredia, N.S., Vizuete, K., Flores-Calero, M., Pazmiño, V.K., Pilaquinga, F., Kumar, B., and Debut, A., 2022, Comparative statistical analysis of the release kinetics models for nanoprecipitated drug delivery systems based on poly(lactic-co-glycolic acid), *PLoS One*, 17 (3), e0264825.

[42] Shafiei, F., Ghavami-Lahiji, M., Jafarzadeh Kashi, T.S., and Najafi, F., 2021, Drug release kinetics and biological properties of a novel local drug carrier system, *Dent. Res. J.*, 18 (1), 94.

[43] Moretto, S., Santos Silva, A., Diaz de Tuesta, J.L., Roman, F.F., Cortesi, R., Bertão, A.R., Bañobre-López, M., Pedrosa, M., Silva, A.M.T., and Gomes, H.T., 2023, Comprehensive characterization and development of multi-core shell superparamagnetic nanoparticles for controlled delivery of drugs and their kinetic release modelling, *Mater. Today Chem.*, 33, 101748.

[44] Hussain, M.A., Rana, A.I., Haseeb, M.T., Muhammad, G., and Kiran, L., 2020, Citric acid cross-linked glucuronoxylans: A pH-sensitive polysaccharide material for responsive swelling-deswelling vs various biomimetic stimuli and zero-order drug release, *J. Drug Delivery Sci. Technol.*, 55, 101470.

[45] Nguyen, M.H., Tran, T.T., and Hadinoto, K., 2016, Controlling the burst release of amorphous drug–polysaccharide nanoparticle complex via crosslinking of the polysaccharide chains, *Eur. J. Pharm. Biopharm.,* 104, 156–163.